3rd National Congress on Physical Sciences, 29 Sep. – 2 Oct. 2016, Sofia
Section: Radiophysics, Electronics and Quantum Electronics

Lidar Investigations of Atmospheric Aerosols over Sofia

T. Dreischuh, A. Deleva, Z. Peshev, I. Grigorov, G. Kolarov, D. Stoyanov

Institute of Electronics, Bulgarian Academy of Sciences,
Sofia 1784, Bulgaria

Abstract. An overview is given of the laser remote sensing of atmospheric aerosols and related processes over the Sofia area performed in the Institute of Electronics, Bulgarian Academy of Sciences, during the last three years. Results from lidar investigations of the optical characteristics of atmospheric aerosols obtained in the frame of the European Aerosol Research Lidar Network, as well as from the lidar mapping of near-surface aerosol fields for remote monitoring of atmospheric pollutants are presented and discussed in this paper.

1 Introduction

Atmospheric aerosols emitted by various natural and anthropogenic sources have been the objective of intensive research in recent decades [1, 2] due to their significant influence on the climate, air quality, and human health [3, 4]. Characterization of the aerosol optical properties could be best done integrating measurements obtained with different active and passive methods, as well as complementary in-situ sensors.

In order to investigate successfully atmospheric aerosol processes, vertical and/or horizontal profiling of aerosol optical parameters is needed. Laser radars (lidars) are widely adopted instruments for active remote sensing of the atmospheric aerosols with high spatial and temporal resolution, high sensitivity and accuracy, covering large distances and observation areas [5, 6].

In this paper we present results obtained in the Laser Radars Laboratory at the Institute of Electronics, Bulgarian Academy of Sciences (LRL-IE) during the last several years, using elastic backscatter lidars for measuring the vertical, horizontal, and temporal distribution of atmospheric aerosols. Lidar remote sensing investigations are performed on days of specific aerosol loadings in the atmosphere, caused by occasionally occurring events such as long-distance trans-border transport of dust from

the Sahara desert and forest fires. Results on lidar mapping of near-surface atmospheric aerosol fields over the city of Sofia and surrounding areas, by scanning in horizontal and vertical directions, are also reported.

2 Sofia Lidar Station

The fast spread of lidar systems contributes to their organizing in lidar networks. The joint analysis of lidar observations in different locations is a useful approach for better understanding and interpretation of some regional aerosol-related events and their influence on the environment. The first aerosol lidar network, established in 2000, with the main goal to provide a comprehensive, quantitative, and statistically significant data base for the aerosol distribution on a continental scale is the European Aerosol Research Lidar Network (EARLINET) [7, 8]. Over the years, the number of EARLINET stations increased from 17 (in 10 countries) in 2000 to 28 stations (in 17 countries) (see Figure 1).

The only lidar station in Bulgaria is located at LRL-IE (42.65N, 23.38E; 590 m above the sea level) in the southeast part of Sofia. Since 2003, it has been involved (as Sofia lidar station) in regular and synchronized lidar measurements of the atmospheric aerosol within the framework of EARLINET, performing systematic lidar monitoring of atmospheric processes [9, 10], unusually high concentrations of aerosols in the troposphere [11], transport of mineral dust from Sahara desert [12], volcanic eruptions [13], formation of smoke layers resulting from forest or industrial fires [14].

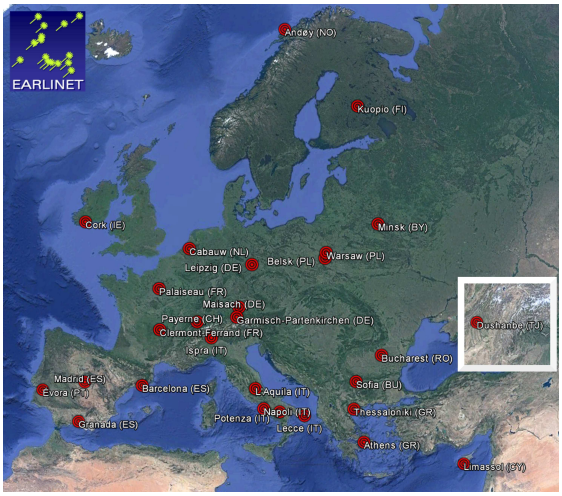

Figure 1: Map of the EARLINET stations currently active. Retrieved October 30, 2016, from `https://www.earlinet.org/index.php?id=121`.

Elastic backscatter lidar systems of the Laser Radar Laboratory, as a part of the EARLINET network, have accomplished tasks of the ACTRIS Research Infrastructure (Aerosols, Clouds, and Trace gasses Research Infra Structure) in the frame of projects supported by the European Commission in the Seventh Framework Programme (project ACTRIS, 1 May 2011 – 30 April 2015) and the Horizon 2020 Research and Innovation Framework Programme (H2020-INFRAIA-2014-2015) (project ACTRIS-2, 1 May 2015 – 30 April 2019).

The lidar systems performing measurements of the aerosol optical parameters are based on CuBr-vapor laser (generating at 510 nm and

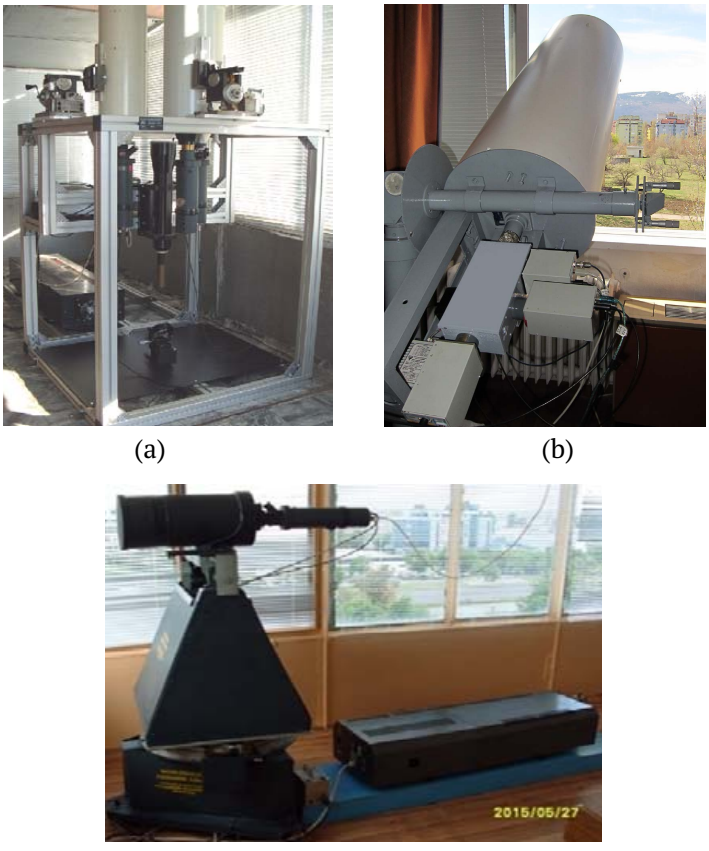

(a) (b)

(c)

Figure 2: Cu-Au-vapor laser (a) and Nd:YAG laser (b) based aerosol lidars at EARLINET Sofia lidar station. Scanning aerosol lidar system employing Cu-vapor laser, used in the investigations of the near-surface aerosol fields (c).

578 nm) and Nd:YAG laser (emitting at 532 nm and 1064 nm). Detailed features of these systems (shown in Figure 2) have been described elsewhere [9].

Despite of the good results obtained during the years, scientific and technological progress leads to the necessity of the respective hardware and software improvements of the lidar systems. In 2015, the CuBr-vapor laser of the first system was replaced by a Cu-Au-vapor laser that significantly expanded the opportunities for a multiwavelength sounding of the atmosphere up to heights of above 15 km, due to the higher average power for each of the generated laser wavelengths (510.6 nm, 578.2 nm and 627.8 nm) and the lower repetition rate of the laser pulses. Lidar measurements performed at two or more wavelengths provide opportunities for better characterizing the optical and, particularly, the microphysical properties of the atmospheric aerosols. This change led to a general transformation of the mechanical construction and the receiving system of the lidar, at the aim to detect simultaneously the backscatter of the three laser wavelengths. The new mechanisms for lidar telescope mounting and adjustments are shown in Figure 2(a).

In 2015, large experimental campaign has been carried out on lidar mapping of near-surface atmosphere over the Sofia urban area. Two scanning lidar systems were used in the aerosol lidar mapping experiments - the Nd:YAG laser-based system shown in Figure 2(b) and Cu-vapor laser-based lidar emitting pulses with a duration of 10 ns at a repetition rate of 5 kHz and wavelengths of 510.6 nm and 578.2 nm, given in Figure 2(c).

3 Lidar Measurements of atmospheric Aerosol Load above Sofia during Saharan Dust Intrusion on 7 April 2016

Every year extremely large amounts of mineral dust (nearly 200-300 million tons) are transported from North Africa to Europe [15, 16]. The basic source of this type of aerosols is the Sahara Desert having an area comparable to that of the European continent and the deepest atmospheric boundary layer (ABL) reaching 5–6 km [17–19]. The atmospheric dust transport is seasonally dependent, exhibiting highest intensity during the spring and summer [20, 21].

Lidar measurements of the atmospheric aerosol loading during Saharan dust intrusions is a basic part of the LRL-IE activities in the last decade, conducted in the frame of the working program of the European Aerosol Lidar Network [22, 23]. In this Section, we describe experimental results obtained on 7 April 2016 by using simultaneous sounding of the atmosphere with two lidars of the laboratory. The measurements are carried out in the approximate time interval 17:00-18:20 UTC (20:00-21:20 local time).

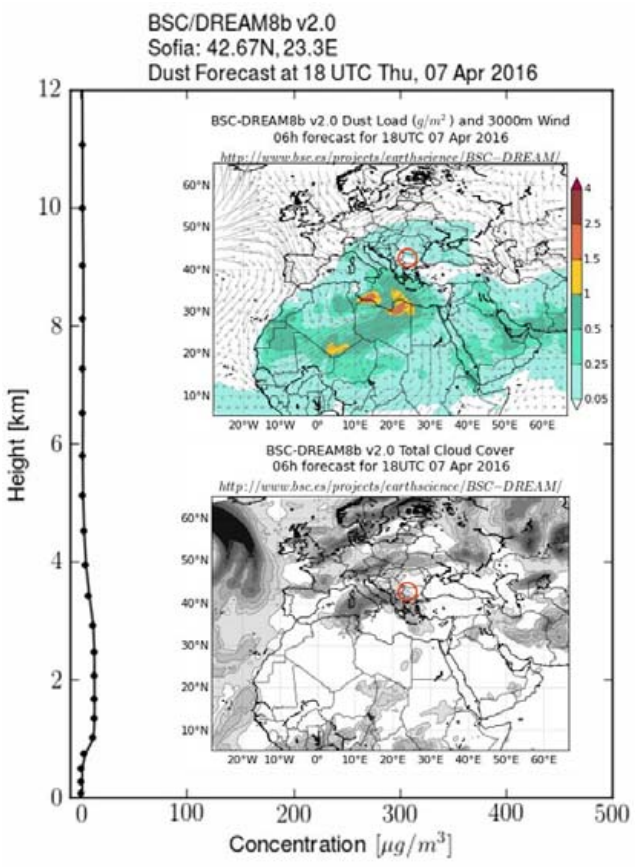

Figure 3: BSC-DREAM8b model forecast of Saharan dust load and cloud cover above Bulgaria on 7 April 2016. The Sofia region is marked by red circles on the maps.

The information provided by the BSC-DREAM8b and HYSPLIT models is used to determine the origin of the registered aerosol layers. According to the BSC-DREAM8b model, a Saharan dust intrusion had taken place above Bulgaria (see color map on Figure 3; the Sofia region is denoted by a red circle). The model forecast for the vertical distribution of the Saharan dust concentration in the atmosphere above Sofia is presented at the left-hand side plot in Figure 3. As this plot shows, dust aerosols have extended mostly within the height interval 1-4 km. Cloud cover over Bulgaria near the time of measurements can be seen on the black-and-white map in Figure 3.

The temporal evolution of the registered aerosol field mass distribution

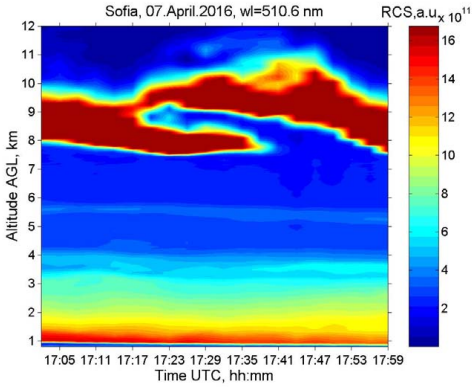

Figure 4: RCS color map of vertical aerosol-density temporal evolution above Sofia, as measured at wavelengths 510.6 nm; height resolution 30 m; temporal resolution 3 min.

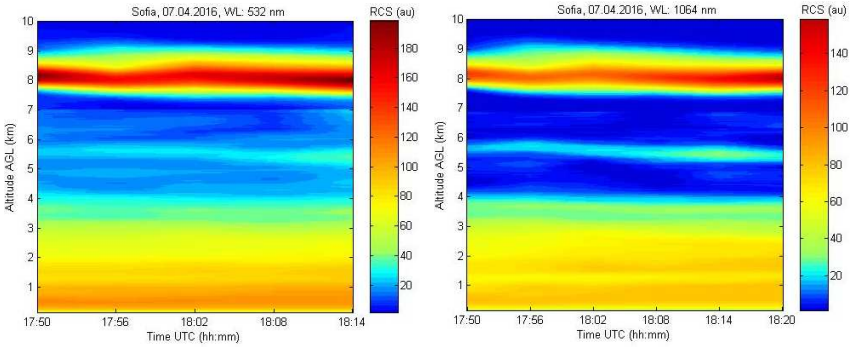

(a) (b)

Figure 5: RCS color maps of vertical aerosol-density temporal evolution above Sofia, as measured at wavelengths 532 nm (a) and 1064 nm (b); height resolution 7.5 m; temporal resolution 5 min.

during the measurements, is displayed as color maps of range-corrected lidar signals (RCS) at the wavelength of 510.6 nm (Figure 4), 532 nm and 1064 nm (Figure 5), respectively.

The RCS color maps show that on 7 April 2016 several aerosol layers are detected – a thick one extended from the ground up to 4 km, a thin aerosol layer at a height of about 5.5 km, and an aloft layer in the altitude range 8–10 km.

We calculated and analyzed a number of HYSPLIT backward trajectories throughout the troposphere in order to explain the aerosol vertical distri-

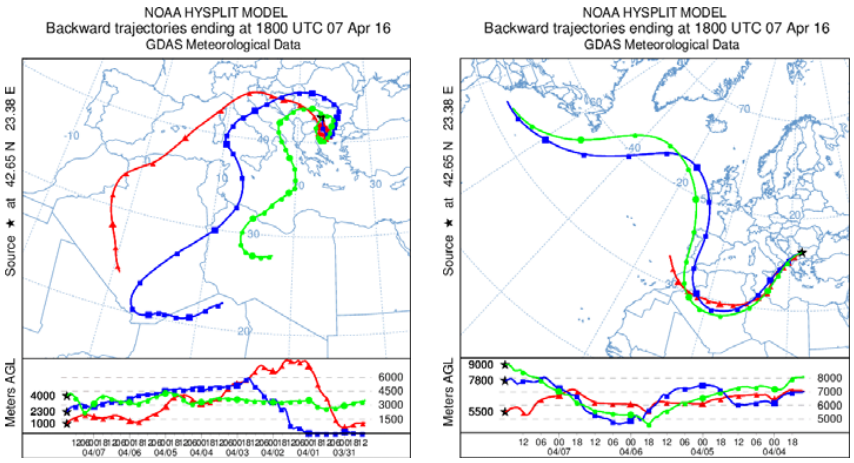

(a) (b)

Figure 6: HYSPLIT-backward trajectories ending above Sofia during the measurements on 7 April 2016.

bution. Some of them are shown in Figure 6. Trajectories delineate the air mass transport pathway prior to reaching Sofia at the time of measurements.

Trajectories ending above Sofia at heights of 1000, 2300, 4000, calculated for a 200-hour period are presented in Figure 6(a). These were chosen so as their endpoints over Sofia to be located nearly uniformly in the range 1–4 km, where the Saharan dust concentration has been considerable, according to the BSC-DREAM forecast (see the left-hand side of Figure 3).

The backward trajectories displayed on Figure 6(a) indicate that, prior to reach Sofia region, the air-masses at the specified altitudes have been moving continuously low above or close to the Sahara Desert surface, whereupon they have passed through dust containing atmospheric domains over the Mediterranean. Therefore, a conclusion can be derived that the observed aerosol loading of the atmosphere in the altitude range 1-4 km above Sofia on 7 April 2016 results mostly from a long-range transport of Saharan mineral dust.

Figure 6(b) presents trajectories ending above Sofia at heights of 5500, 7800 and 9000 m calculated for a 100-hour period. These are chosen because their endpoints nearly correspond to the heights of the observed aerosol layers above 4km, as can be seen on the RCS maps in Figures 4 and 5. The obtained backward trajectories show that the air-masses at these altitudes have passed consecutively over the Atlantic Ocean, Sahara Desert, dust-rich atmospheric regions over the Mediterranean, de-

scending during the transport down to a height of about 5 km. Taking into account the presented backward trajectories and the mentioned above high top boundary of the Saharan ABL, one can presume that the air-masses at the regarded altitudes above 4 km have contained considerable amounts of humid air, other type general aerosols, and, possibly, some small amounts of Saharan dust. This is in accordance with the BSC-DREAM8b model dust concentration profile shown in Figure 3, indicating absence or very low concentration of dust above 4 km at the time of measurements. If present, some dust particles at the regarded altitudes could serve as condensation nuclei in forming the clouds above 4 km.

4 Lidar Mapping of Urban Aerosols

The aerosol mapping by means of scanning elastic-scattering lidars is a fast and effective approach to detecting polluting aerosol loads over broad densely populated or industrial areas, as well as to determining aerosol density, spatial distribution, and temporal dynamics [24–26]. Results on lidar mapping of near-surface atmospheric aerosol fields over the city of Sofia and surrounding areas, by scanning in horizontal and vertical directions, will be shortly presented in this Section. An extensive lidar data set is obtained during a seven-month experimental campaign in 2015, carried out in the frame of a common project with Sofia Municipality. A more detailed presentation of the results has been reported elsewhere [27].

Two types of lidar scanning measurements have been performed: vertical scanning at a fixed azimuth angle, changing at the same time continuously the elevation angle, and horizontal scanning at a fixed elevation angle, changing the azimuth angle. The aerosol mapping in North and North-West (N-NW) direction (toward Stara Planina mountain and the central parts of Sofia) by using the lidar equipped with a Cu-vapor laser (located on the top of the building of the Institute of Electronics) can be accomplished at an elevation angle of 0°. For the measurements in South - South-West (S-SW) direction (toward Vitosha mountain), performed by using the Nd:YAG laser-based lidar, a low elevation angle ($6–7^\circ$) was used because of the presence of high buildings and trees in this direction.

Range profiles of the aerosol backscattering and extinction coefficients are the aerosol parameters derived from raw lidar data on the basis of so-called lidar equation describing the relation between the received range-resolved backscattered optical radiation power and atmospheric and system parameters [5, 6]. At the next step of processing the aerosol backscatter profiles resulting from horizontal or vertical scanning, two-dimensional color-coded sector maps of the near-surface aerosol density are obtained. Red coloring corresponds to higher aerosol density, while

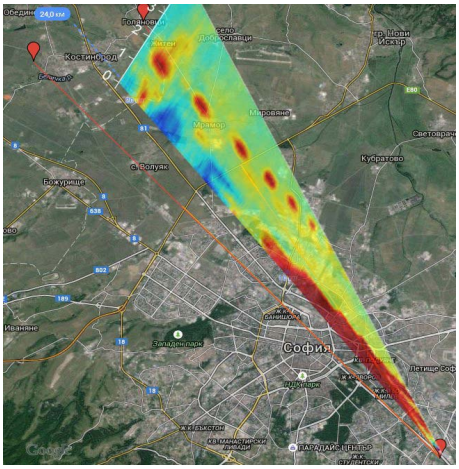

Figure 7: Vertical distribution of the aerosol backscattering coefficient obtained along a fixed azimuth of 326° with respect to the North.

the blue one – to lower aerosol density. In the next figures, the obtained color maps are presented overlaid onto a Google map of the investigated area.

The vertical lidar scanning is used to acquire information about the vertical structure of the aerosol concentration. Figure 7 shows a range-height color map constructed using lidar profiles (averaged over five individual scans) obtained along a fixed azimuth (326° with respect to the North clockwise) at different elevation angles (0–10°), with an increment of 1°. A well pronounced vertical layer near ground surface (close to a thoroughfare with intense traffic) was observed in the height range 500–700 meters. Aerosol formations were detected at a height of ~ 1–2 km above ground, with a density higher than that of the surrounding atmosphere, probably low clouds. This vertical map demonstrates the capability of such a type lidar measurements to determine quickly and precisely the location of the sources of anthropogenic particular matter emissions in the atmosphere. On the other hand the horizontal-scanning lidar measurements, provide significant information about the air pollution by near-ground surface aerosol fields.

Figure 7 illustrates also the operational distance of the lidar measurements performed. The maximum distance exceeded 20 km, limited by the high laser pulse repetition rate, in the case of Cu-vapor lidar, and by the surface topology of the observation area in S-SW direction, in the case of Nd:YAG lidar.

Results of horizontal lidar scanning measurements and mapping of the

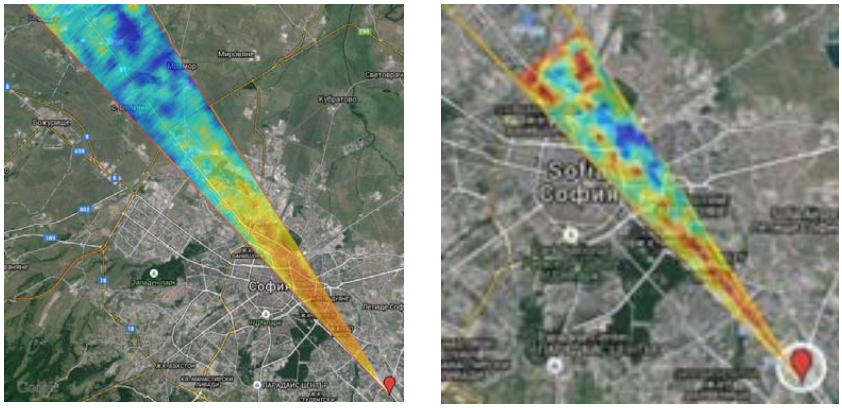

(a) (b)

Figure 8: Horizontal aerosol density distribution as measured on 6 August 2015 in the time interval 21:33-22:10 LT, at distances of more than 20 km (a) and on 23 July 2015 in the time interval 21:33-22:10 LT, at distances of up to 10 km (b).

near-surface aerosols in the atmosphere above Sofia and the surrounding areas are presented below.

Figure 8 show results of lidar mapping in NW direction, including the central parts of the city. They were performed by the lidar equipped with a Cu-vapor laser at the wavelength of 510.6 nm. The near-surface aerosol density distribution, resulting from measurements carried out on 6 August 2015, in the interval 21:33-22:10 local time (LT), is presented in Figure 8(a).

The investigated azimuth sector of 8.5° covered the central city zones including and being nearly parallel to one of the main city thoroughfare, reaching distances of near 22 km. Due to the heavy city traffic, relatively higher values of the aerosol backscattering, and, respectively, the aerosol density were observed over the urban areas reaching the city ring road. At distances beyond the ring road, the aerosol pollution concentration is lower (see the blue-colored areas), so we could assume that the aerosol fields observed by the lidar were of anthropogenic origin.

In Figure 8(b), results are presented of lidar measurements performed in the time interval 21:36 – 22:09 on 23 July 2015. The lidar sounding was directed NW to distances of 10 km, covering mainly the central parts of the city. Areas of relatively higher aerosol pollution were observed, mainly close to the busy streets, but also over some densely populated residential districts (yellow-brown colored areas on the map).

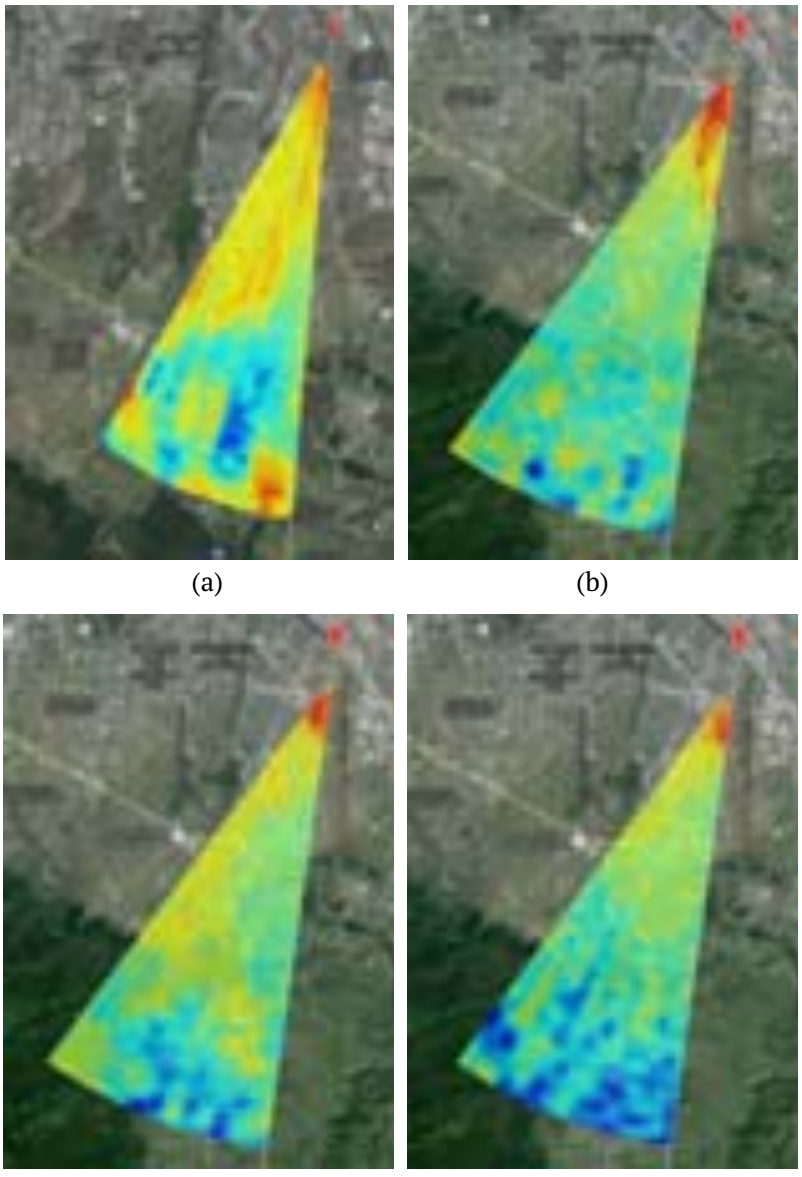

(a) (b)

(c) (d)

Figure 9: Temporal variations of the aerosol density distribution: Results from the lidar scanning measurements performed in an azimuth sector of 28° on 9 November 2015 in the time intervals 10:23–11:40 LT (a), 18:12–19:07 LT (b), 19:10–20:10 LT (c), and 20:12–21:01 LT (d).

Figure 9 demonstrates the capability of lidar scanning methods to determine not only the aerosol density and spatial distribution, but also the temporal variations of the aerosol density distribution. On 9 November 2015 four measurements were performed in the same angular sector of 28° - one daytime over distances of up to 6 km and three successive nighttime ones over distances of up to 9 km.

The daytime measurement data Figure 9(a) show presence of aerosol fields characterized by relatively high density and nearly homogeneous distribution (predominantly colored in red-yellow on the map) above the city part close to the lidar up to the city ring road (distances of up to 3.5–4 km). Over some residential districts close to the ring road (left-side part of the observation sector), a zone of low aerosol concentration has been formed, passing farther to one of even lower aerosol densities when approaching the mountain foot. In that remote part of the lidar-mapped zone, separate spots of higher or lower aerosol concentration could also be observed.

Juxtaposing the three color maps corresponding to the three successive 1-hour lasting evening measurements (Figures 9(b-c)) reveals occurrence of highest aerosol densities in the near to the lidar station zone at distances of 1–2 km, as well as moderate dynamics of the aerosol distribution picture over the whole sector of lidar scanning.

5 Conclusions

In this work we briefly presented results of lidar remote sensing of atmospheric aerosols and related processes over the Sofia region performed in the Laser Radars Laboratory at the Institute of Electronics, Bulgarian Academy of Sciences. The investigations are caried out mainly in the framework of the European Aerosol Research Lidar Network.

Reported in the paper multi-wavelength lidar observations on long-distance transport of Saharan dust are confirmed by the BSC-DREAM8b model dust concentration data and the HYSPLIT air-mass backward trajectories. The analysis of the obtained two-dimensional aerosol lidar maps, as overlaid on the topological map, shows a good correlation between the aerosol density distribution and the locations of important sources of aerosol pollution, such as streets with intense traffic, densely populated areas, etc. The last research was performed under a contract with a Sofia Municipality.

Summarazing, the lidar remote sensing of the atmosphere, including the lidar aerosol mapping, appears to be an effective approach to accurate and reliable determination of the presence of atmospheric aerosols and their density, spatial distribution, and temporal dynamics.

Acknowledgments

The financial support for EARLINET in the ACTRIS Research Infrastructure Project by the European Unions Horizon 2020 research and innovation programme under grant agreement n. 654169 and previously under grant agreement n. 262254 in the 7th Framework Programme (FP7/2007-2013) is gratefully acknowledged. This research has also been supported by the Municipality of Sofia. The authors thankfully acknowledge data and images from the BSC-DREAM8b (Dust REgional Atmospheric Model) model, operated by the Barcelona Supercomputing Center (http://www.bsc.es/projects/earthscience/BSC-DREAM/) and the NOAA Air Resources Laboratory for the provision of the HYSPLIT transport and dispersion model and READY website (http://www.ready.noaa.gov) used in this publication.

Bibliography

[1] P.H. McMurry (2000) *Atmos. Environ.* **34** 1959-1999.

[2] M. Chin, R. Kahn, and S. Schwartz (2009) *Atmospheric Aerosol Properties and Climate Impacts: A Report by the U.S. Climate Change Science Program and the Subcommittee on Global Change Research*, NASA, Washington, DC, USA.

[3] S. Fuzzi, et al. (2015) *Atmos. Chem. Phys.* **15** 8217-8299.

[4] World Health Organisation (WHO) (2013) *Review of evidence on health aspects of air pollution - REVIHAAP Project. Technical Report.* WHO Regional Office for Europe, Copenhagen, Denmark.

[5] R.M. Measures (1984) *Laser Remote Sensing*, Wiley, New York, USA.

[6] V.A. Kovalev and W.E. Eichinger (2004) *Elastic Lidar: Theory, Practice, and Analysis Methods*, Wiley, New York, USA.

[7] J. Boesenberg, et al. (2003) *EARLINET: A European Aerosol Research Lidar Network to establish an aerosol climatology*, Technical Report 348, Max Planck Inst. fuer Meteorology, Hamburg, Germany.

[8] G. Pappalardo, et al. (2014) *Atmos. Meas. Tech.* **7** 2389-2409.

[9] D. Stoyanov, et al. (2012) LIDAR Atmospheric Sensing by Metal Vapor and Nd:YAG Lasers, in *Advanced Photonic Sciences*, ed. M. Fadhali, InTech, p. 345.

[10] Z. Peshev, T. Dreischuh, E.Toncheva, and D. Stoyanov (2012) *J. Appl. Remote Sens.* **6** 063581.

[11] A. Deleva and I. Grigorov (2011) *IJNO* **2011** 1-8.

[12] Z. Peshev, T. Dreischuh, Ts. Evgenieva, A. Deleva, D. Tonev, and D. Stoyanov (2016) *J. Appl. Remote Sens.* **10** 036009.

[13] I. Grigorov, D. Stoyanov, and G. Kolarov (2011) *Proc. SPIE* **7747** 77470R.

[14] I. Grigorov, A. Deleva, D. Stoyanov, N. Kolev, and G. Kolarov (2011) *Proc. SPIE* **7747** 77470U.

[15] F. De Tomasi, A. Blanco, and M.R. Perrone (2003) *Appl. Opt.* **42** 1669-1709.

[16] C. Mitsakou, G. Kallos, N. Papantoniou, C. Spyrou, S. Solomos, M. Astitha, and C. Housidas (2008) *Atm. Chem. Phys.* **8** 7181-7192.

[17] L. Garcia-Carreras, D.J. Parker, J.H. Marsham, P.D. Rosenberg, et al. (2015) *J. Atmos. Sci.* **72** 693-713.

[18] J. Cuesta, J. H. Marsham, D. J. Parker and C. Flamant (2009) *Atmos. Sci. Let.* **10** 34 – 42.

[19] M. Gammo (1996) *Bound. Layer Meteorol.* **79** 265-278.

[20] N. Kubilay, S. Nickovic, C. Moulin, and F. Dulac (2000) *Atmos. Environ.* **34** 1293-1303.

[21] P. Alpert, B.U. Neeman, and Y. Shay-El (1990) *JCLI* **3** 1474-1478.

[22] A. Papayannis, V. Amiridis, L. Mona, G. Tsaknakis, et al. (2008) *J. Geophys. Res.* **113** D10204.

[23] A. Papayanis, V. Amiridis, L. Mona, R.E. Mamouri, et al. (2009) *Proc. SPIE* **7479** 74790C.

[24] S.M. Spuler and Sh.D. Mayor (2007) *Proc. SPIE* **6681** 668102.

[25] F. Gao, K. Bergant, A. Filipcic, B. Forte, D.-X. Hua, X.-Q. Song, S. Stanic, D. Veberic, and M. Zavrtanik (2011) *J. Quant. Spectrosc. Radiat. Trans.* **112** 182-188.

[26] T.-Y. He, S. Stanic, F. Gao, K. Bergant, D. Veberic, X.-Q. Song, and A. Dolzan A. (2012) *Atmos. Meas. Tech.* **5** 891-900.

[27] T. Dreischuh, I. Grigorov, Z. Peshev, A. Deleva, G. Kolarov, and D. Stoyanov (2016) *Lidar Mapping of Near-Surface Aerosol Fields*, in: *Aerosol*, ed. K. Volkov; InTech, Rijeka, Slovenia, ISBN 978-953-51-4963-7 (accepted).